Supporting Information

Preparation of polymer brush grafted anionic or cationic silica nanoparticles – systematic variation of the polymer shell

Marek Sokolowski,*[1] Christoph Bartsch,[1] Vivian J. Spiering,[1] Sylvain Prévost,[2], Marie-Sousai Appavou,[3] Ralf Schweins,[2] Michael Gradzielski*[1]

[1] Stranski Laboratorium für Physikalische Chemie, Technische Universität Berlin, Straße des 17 Juni 124, 10623 Berlin, Germany

[2] Institut Laue - Langevin, DS / LSS, 71 Avenue des Martyrs, 38042 Grenoble CEDEX 9

[3] Jülich Center for Neutron Scattering JCNS at Heinz Maier-Leibnitz-Zentrum (MLZ), Forschungszentrum Jülich GmbH, Lichtenbergstraße 1, 85748 Garching, Germany

1 Synthesis

1.1 SiO_2-NP-synthesis

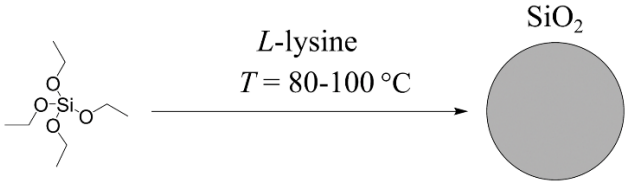

Figure S1. Scheme of lysine catalyzed synthesis from TEOS to SiO_2-NPs.

For exactly reproducible results always a similar stirring procedure should be used due to the influence in the nucleation and growth properties of the silica nanoparticles as a result of the convection properties in the reaction mixture. Faster stirring rates reduce the effective NP size. A 250 mL round bottom flask was used and stirrer metrices were:

- length: 2 cm
- diameter: 0.5 cm

Table S1. Reaction time, mixture temperature *T*, mass of *L*-lysine and adjusted stirrer speed for the desired size of the SiO_2-NP

d_{NP}	reaction time	*T*	stirrer speed	*L*-lysine
nm	h	°C	RPM	g
50	36	90	270	0.062
70	40	90	250	0.062
140	27	105	100	0.074

1.2 SiO_2@NH_2-synthesis

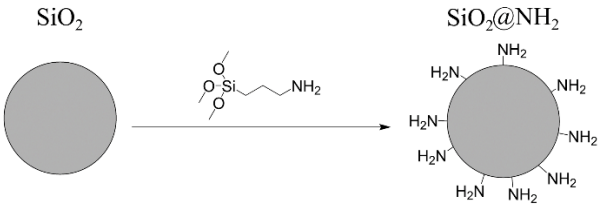

Figure S2. Surface modification of bare SiO_2 to SiO_2@NH_2.

Table S2. Concentration, mass of APTS and acetic acid for the amino surface modification with APTS

d_{NP}	*C* (SiO_2)	*m* (APTS)	*m* (acetic acid)
nm	wt%	g	g
50	1.28	1.3	4
70	1.34	1.3	4
140	3.00	1.3	4

1.3 SiO_2@Br-synthesis

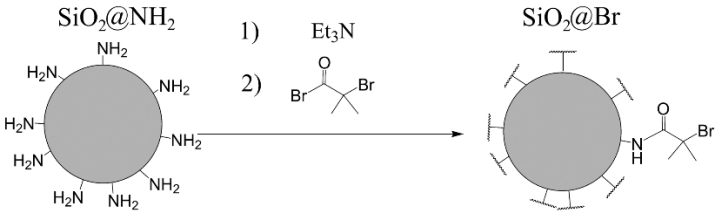

Figure S3. Surface initiated modification with 2-bromo-2-methylpropionyl bromide (BIBB).

1.4 SiO_2@PDMAEMA

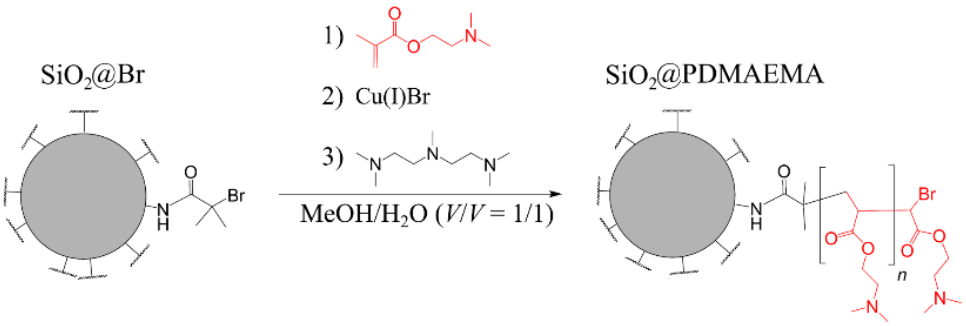

Figure S4. Polymerization via ATRP with monomer DMAEAMA.

1.5 SiO_2@P*t*BUMA

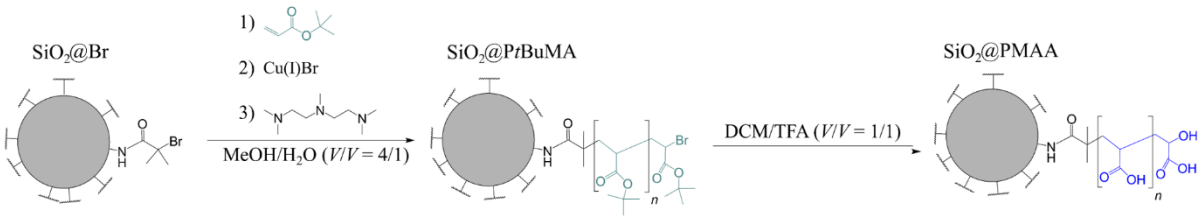

Figure S5. Polymerization via ATRP with monomer *t*BuMA.

Table S3. Weight fractions *m* for ATRP for polymerization of DMAEMA and *t*BuMA, the theoretical mass ratio of polymer (for 100 % conversion) and silica *m*(P)/*m*(NP), and measured grafted amount of polymer from TGA results corresponding to the mass of grafted polymer *m* (grafted)

d_{NP} nm	*m*(P)/*m* (NP)	*M* (DMAEMA) g	grafted polymer wt%	*m* (grafted) mg	*m*(P)/ *m*(NP)	*m* (*t*BuMA) g	grafted polymer wt%	*m* (grafted) mg
	SiO_2@PDMAEMA				**SiO_2@PMAA**			
50	2.37	0.05	3.0	0.6	4.23	0.0711	2.5	0.5
50	3.47	0.09	4.5	1.0	8.46	0.1422	3.0	0.6
50	7.74	0.16	5.5	1.2	16.9	0.2844	7.5	1.7
50	15.48	0.31	7.0	1.6	25.39	0.4266	10.5	2.5
50	38.42	0.79	11.5	2.7	33.85	0.5688	13.0	3.1
50	–	–	–	–	42.32	0.7110	14.5	3.6
70	2.37	0.05	17.5	4.5	4.23	0.0711	4.5	1.0
70	3.47	0.09	20.5	5.4	8.46	0.1422	5.5	1.2
70	7.74	0.16	23.5	6.5	16.9	0.2844	7.0	1.6
70	15.48	0.31	27.5	8.0	25.39	0.4266	7.8	1.8
70	38.42	0.79	28.5	8.4	33.85	0.5688	8.0	1.8
70	–	–	–	–	42.32	0.7110	13.5	3.3
140	2.37	0.05	27.5	8.0	4.23	0.0711	1.5	0.3
140	3.47	0.09	27.5	8.2	8.46	0.1422	4.5	1.0
140	7.74	0.16	28.1	8.2	16.9	0.2844	5.5	1.2
140	15.48	0.31	31.5	9.7	25.39	0.4266	6.5	1.5
140	38.42	0.79	33.5	10.6	33.85	0.5688	7.0	1.6
140	–	–	–	–	42.32	0.7110	4.0	1.0

m(SiO_2@Br, *d* = 50 nm) = 0.021 g
m(SiO_2@Br, *d* = 70 nm) = 0.021 g
m (SiO_2@Br, *d* = 1400 nm) = 0.021 g
m(Cu(I)Br) = 0.055 g (0.38 mmol)
V(PMDETA) = 73 µL (0.34 mmol)

For SANS-samples: Several reaction batches of polymer grafted NPs were combined and condensed with a rotary evaporator by simultaneously applying continuous sonication to increase the concentration as much as possible. Condensed NPs were filtered with a 5 µm cellulose acetate filter and treated with ultrasounds (tip finger) for one minute. The remaining solution was diluted with deuterium oxide to the desired V_{D2O}/V_{H2O} ratio.

2 Surface modification – Molecular weight

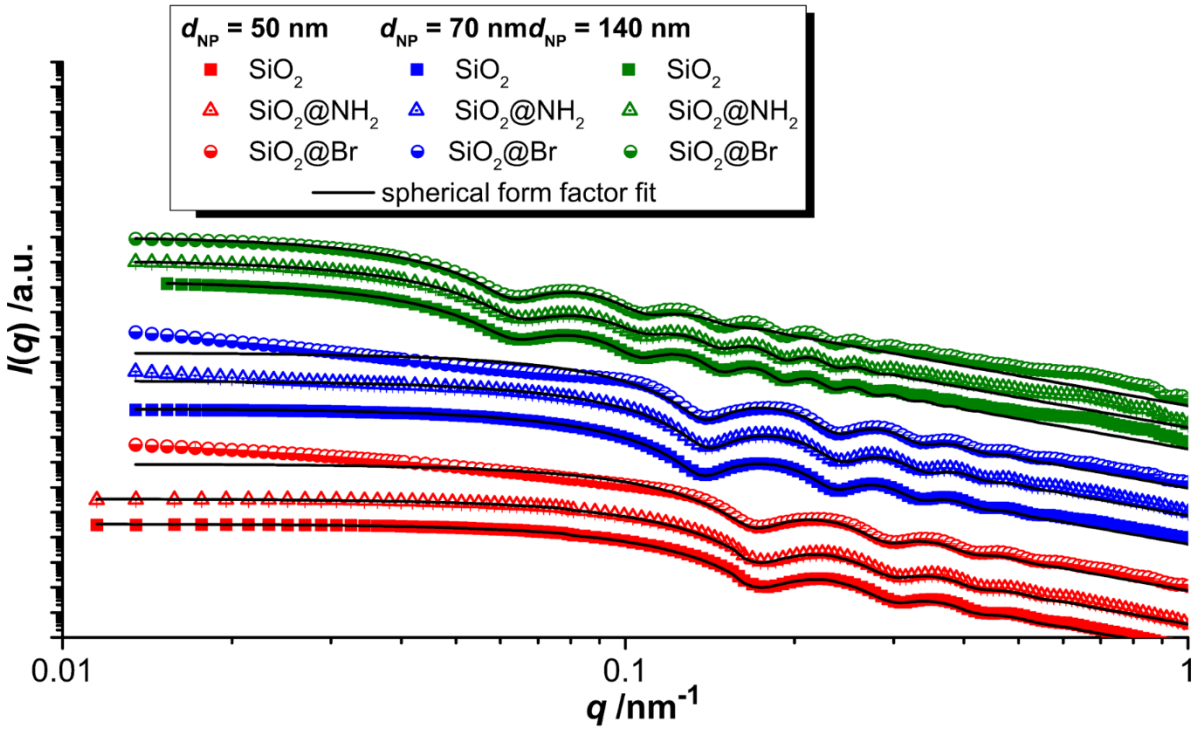

Figure S6. Shown is SAXS-data of all NP modifications.

As the major objective was to obtain stable colloidal solution with the smallest amount of aggregated NPs after each functionalization all surface modified NPs were analyzed with scattering techniques (LS, SAXS) and additionally with ζ-potential measurements. For SAXS all data were fitted using a spherical form factor respecting the particle number density and scattering length density difference of $\Delta SLD = 9.5 \cdot 10^{-4}$ nm^2 (with $SLD_{water}=9.4 \cdot 10^{-4}$ and $SLD_{SiO2}=18.9 \cdot 10^{-4}$ nm^{-2}, considering $\rho_{SiO2}=2.2$ g·cm^{-3}) For all NPs the PDI is remarkably low indicating that size and polydispersity are well controlled via *L*-lysine modified NP synthesis. For SAXS-measurements concentrations were adjusted to 0.2 wt%. However, we measured the exact concentration after the measurement by means of evaporating the solvent. The data show that the small SiO_2@Br-NPs (d = 50 and 70 nm) have an additional upturn in the low q-regime indicating aggregation. Thus we interpreted a colloidal stability loss during solvent transfer from polar to unpolar conditions as a result of reduced electrostatic stabilization. Attaching the Br-moiety reaction leads to a reduce surface potential (ionizable NH_2-moieties are replaced by uncharged Br-moities) of less than 25 mV (table S4), which is usually considered to be a threshold for colloidal stability. For the subsequent polymerization the majority of those aggregates can be separated into single NPs again by sonication and once NPs are charged due to polymer protonation or deprotonation long time colloidal stable solutions can be achieved as long ζ-potentials are high.

Table S4. Measured data SiO_2-, SiO_2@NH_2, SiO_2@Br-NPs; for light scattering: hydrodynamic radii R_H, extrapolated with Guinier approximation forward scattering $I_{0,LS}$, weight concentration $c_{g,LS}$, and molecular weight $M_{W,LS}$; for SAXS: weight concentration $c_{g,SAXS}$, approximated forward scattering $I_{0,SAXS}$, radius of the core R_{NP}, the polydispersity index PDI, the molecular weight $M_{W,SAXS}$, theoretical molecular weight $M_{W,th}$ calculated from the radius, relative deviation of measured (SAXS data) and theoretical molecular weight and the ζ-potential data at high charged conditions.

		LS data				SAXS data							
d_{theo}	surface modification	R_H	$I_{0,LS}$	c_g	$M_{W,LS}$	$c_{g,SAXS}$	$I_{0,SAXS}$	R_{NP}	PDI	$M_{W,SAXS}$	$M_{W,th}$	1-$M_{W,SAXS,R}$/$M_{W,th}$	ζ
nm		nm	cm^{-1}	g/L	g/mol	g/L	cm^{-1}	nm		g/moL	g/moL		mV
50	–OH	29	0.00540	0.3	6.98E+08	2.2	591	24.3	0.086	8.69E+07	7.96E+07	0.06	–54.3
50	–NH2	34	0.00540	0.5	4.64E+08	2.2	595	24.3	0.086	8.75E+07	7.96E+07	0.07	+49.0
50	–Br	73	0.07848	0.4	9.11E+09	2.3	–	24.4	0.088	–			–24.1
70	–OH	36	0.01065	2.0	2.24E+08	2.1	1337	32.6	0.074	2.06E+08	1.92E+08	0.05	–46.9
70	–NH2	37	0.01384	2.0	2.91E+08	2.1	1286	32.5	0.072	1.98E+08	1.91E+08	0.02	+43.8
70	–Br	82	0.01753	3.1	2.40E+08	2.2	–	32.6	0.080	–			–21.2
140	–OH	73	0.04921	1.0	2.26E+09	2.2	14440	70.3	0.070	2.12E+09	1.93E+09	0.09	–55.4
140	–NH2	74	0.05814	1.0	2.44E+09	1.9	12649	70.3	0.073	2.15E+09	1.93E+09	0.09	+53.2
140	–Br	74	0.05108	1.3	1.71E+09	1.8	10766	70.3	0.070	1.93E+09	1.93E+09	-0.01	–20.5

Molecular weight of the silica core

The value for $M_{W,NP}$ is calculated from the forward scattering I_0 from the SAXS-data via:

$$M_{W,NP} = \frac{N_A I_0 \rho_{SiO_2}^2}{\Delta\eta^2 \cdot c_g} \quad (3)$$

For example, NPs diameter of d = 50 nm:

$$M_{W,NP} = \frac{6.022 \cdot 10^{23} \frac{1}{mol} \cdot 591 \frac{1}{cm} \cdot \left(2.2 \frac{g}{cm^3}\right)^2}{\left(9.49 \cdot 10^{10} \frac{1}{cm^2}\right)^2 \cdot 0.0022 \frac{g}{cm^3}} = 8.694 \cdot 10^7 \frac{g}{mol} \quad (3)$$

Complementary the theoretical molecular weight can also be calculated via the radii obtained for the spherical particles as:

$$M_{W,SAXS,R} = \frac{N_A 4\pi R^3 \rho_{SiO_2}}{3}(1 + 3PDI^2) \quad (3b)$$

Refractive Index Increment

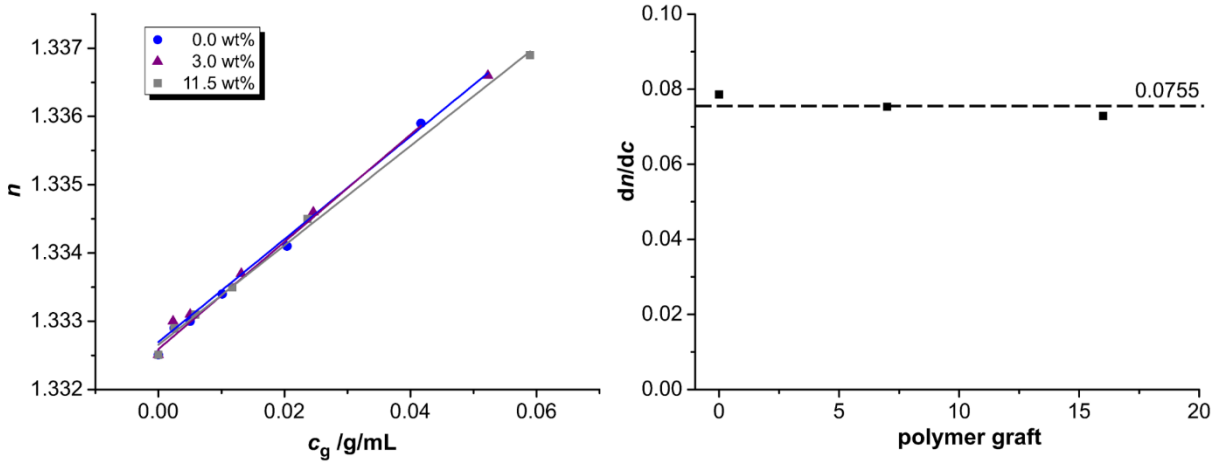

Figure S7. Measured refractive index n of silica nanoparticle solution d = 50 nm with different polymer grafting as a function of the NP weight concentration. Measured data collected from the wavelength of red light bulb (closely simulating the wavelength of a laser light λ = 632.8 nm).

As dn/dc is almost identical the average dn/dc is calculated with dn/dc = 0.0755 mL/g.

3 TGA

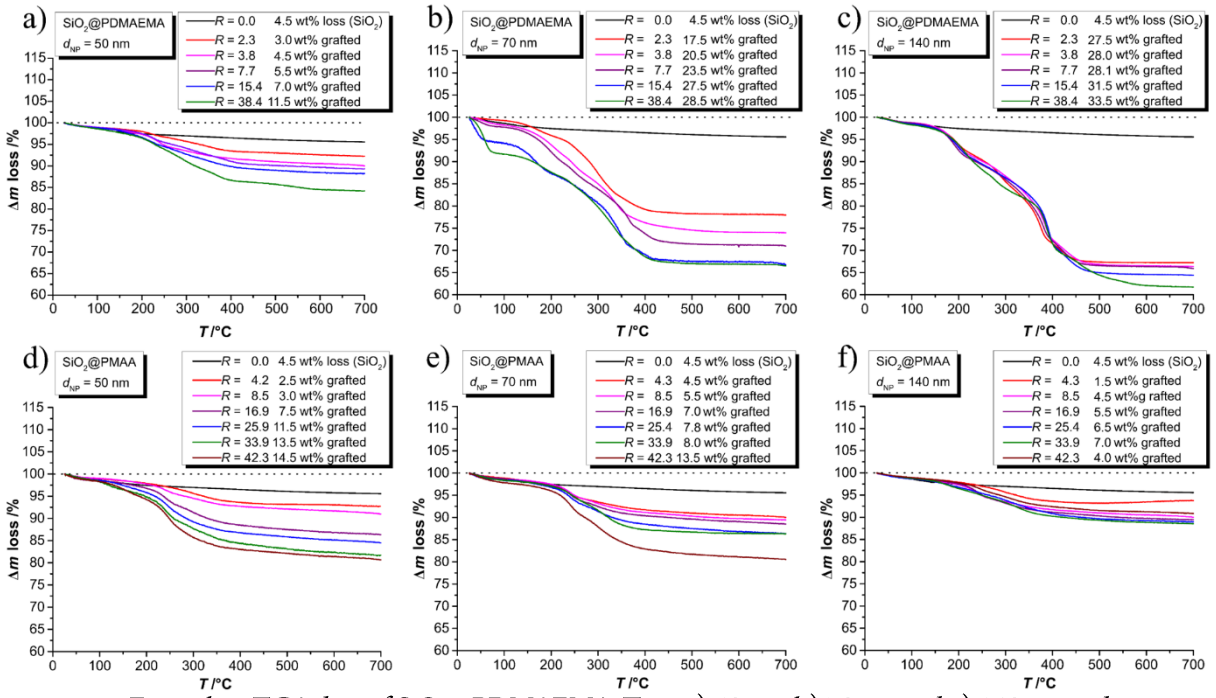

Figure S8. Exemplary TGA data of SiO_2@PDMAEMA. Top; a) 50 nm, b) 70 nm and c) 140 nm and SiO_2@PMAA (bottom; d) 50 nm, e) 70 nm and f) 140 nm.

<u>Calculation of the molecular weight of polymer grafted NPs</u>

First, we determined the weight loss from the pure SiO_2-NPs which can be attributed to the loss of tightly bound water. From this we can determine a fraction x of the initial mass of the SiO_2-NPs, that was water via the relation:

$$\Delta m(\mathrm{SiO_2}, 25\ °\mathrm{C}) = \Delta m(\mathrm{SiO_2}, 700\ °\mathrm{C}) \cdot (1 + \mathrm{x}) \qquad \text{(S1)}$$

where for our case x was determined to be 0.047. Then, the absolute molecular weight of polymer grafted $M_{W,NP+P}$ was determined by multiplying the $M_{W,NP}$ of the core (obtained from SAXS via eq. 3, Table S4) with the polymer percentage obtained from TGA $\Delta m_{polymer}$:

$$M_{W,NP+P} = M_{W,NP} \cdot \left(\frac{m(25\ °C)}{m(700\ °C)} - x\right) \qquad \text{(S2)}$$

where m(25 °C) is the mass of the polymer containing sample at the beginning of the experiment and m(700 °C) at the end of the experiment.

<u>Example calculation</u>

For Silica a measured value is 95.5 %.

$$x = \frac{\Delta m(\mathrm{SiO_2}, 25\ °\mathrm{C})}{\Delta m(\mathrm{SiO_2}, 700\ °\mathrm{C})} - 1 = \frac{100\ \%}{95.5\ \%} - 1 = 0.047 \qquad \text{(S1)}$$

Now the fraction of tightly bound water is 0.047.

For example, SiO_2@PDMAEMA with 3.0 wt% grafted polymer for core diameter 50 nm have a measured value at 700 °C:

SiO_2@PDMAEMA 92.5 %

and with equation S2 the molecular weight is:

$$M_{W,NP+P} = 8.69 \cdot 10^7 \frac{g}{mol} \cdot \left(\frac{100\,\%}{92.5\,\%} - 0.047\right) = 8.99 \cdot 10^7 \frac{g}{mol}. \quad (S2)$$

Table S5. Parameter from the TGA investigation for SiO_2@PDMAEMA and SiO_2@PMAA-NPs: monomer concentration *c*(monomer), expected mass loss if 100% monomer conversion would have taken place, TGA theoretical for 100 % conversion, measured data mass loss, TGA experimental, and the corresponding conversion rate of the monomer (conversion = TGA experimental/TGA theoretical).

d_{core}	SiO_2@PDMAEMA				SiO_2@PMAA			
[nm]	*c*(monomer)	TGA data	TGA theo	conversion	*c*(monomer)	TGA data	TGA theo	conversion
	mM	%	%	%	mM	%	%	%
50	0.3	3.0	70.4	4.3	0.5	2.5	65.6	3.8
50	0.6	4.5	81.1	5.5	1.0	3.0	79.2	3.8
50	1.0	5.5	88.2	6.2	2.0	7.5	88.4	8.5
50	2.0	7.0	93.7	7.5	3.0	10.5	92.0	11.4
50	5.0	11.5	97.4	11.8	4.0	13.0	93.8	13.9
50	–	–	–	–	5.0	14.5	95.0	15.3
70	0.3	17.5	70.4	24.9	0.5	4.5	65.6	6.9
70	0.6	20.5	81.1	25.3	1.0	5.5	79.2	6.9
70	1.0	23.5	88.2	26.6	2.0	7.0	88.4	7.9
70	2.0	27.5	93.7	29.3	3.0	7.8	92.0	8.5
70	5.0	28.5	97.4	29.3	4.0	8.0	93.8	8.5
70	–	–	–	–	5.0	13.5	95.0	14.2
140	0.3	27.5	70.4	24.9	0.5	1.5	65.6	2.3
140	0.6	28.0	81.1	25.3	1.0	4.5	79.2	5.7
140	1.0	28.1	88.2	26.6	2.0	5.5	88.4	6.2
140	2.0	31.5	93.7	29.3	3.0	6.5	92.0	7.1
140	5.0	33.5	97.4	29.3	4.0	7.0	93.8	7.5
140	–	–	–	–	5.0	4.0	95.0	4.2

4 ζ-potential values

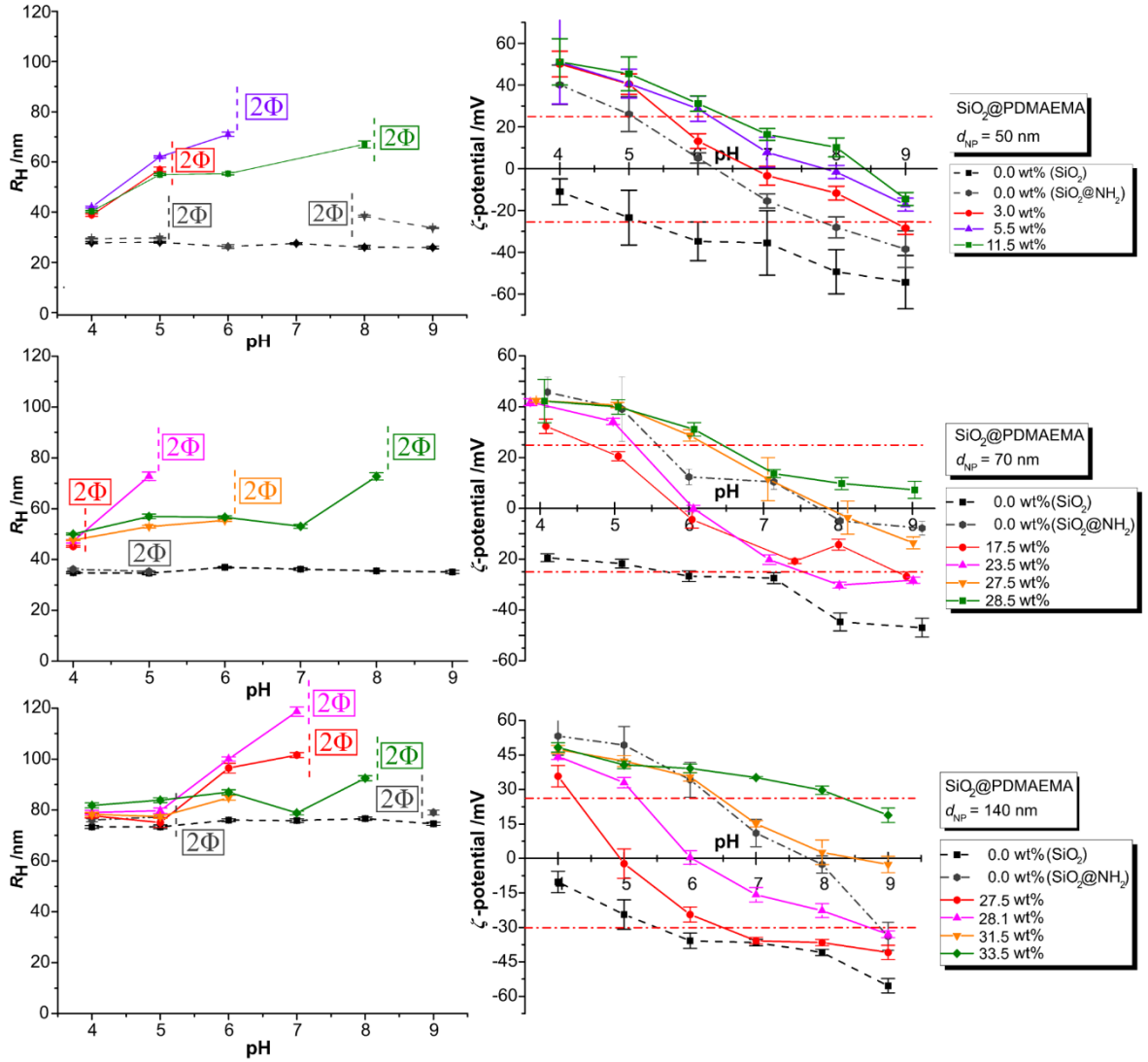

Figure S9. pH dependent values for hydrodynamic radii R_H (left) and ζ-potentials for all SiO_2@PDMAEMA-NPs (top $d = 50$ nm, middle $d = 70$ nm, bottom, $d = 140$ nm).

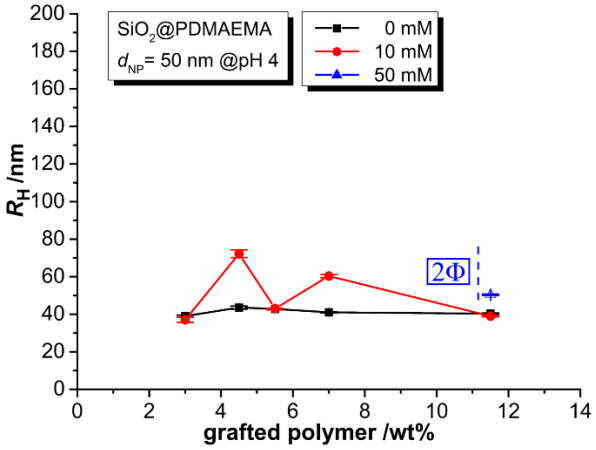

Figure S10. Hydrodynamic radii R_H for SiO_2@PDMAEMA-NPs with $d = 50$ nm as a function of the amount of grafted polymer for different ionic strengths (NaCl) at 25 °C.

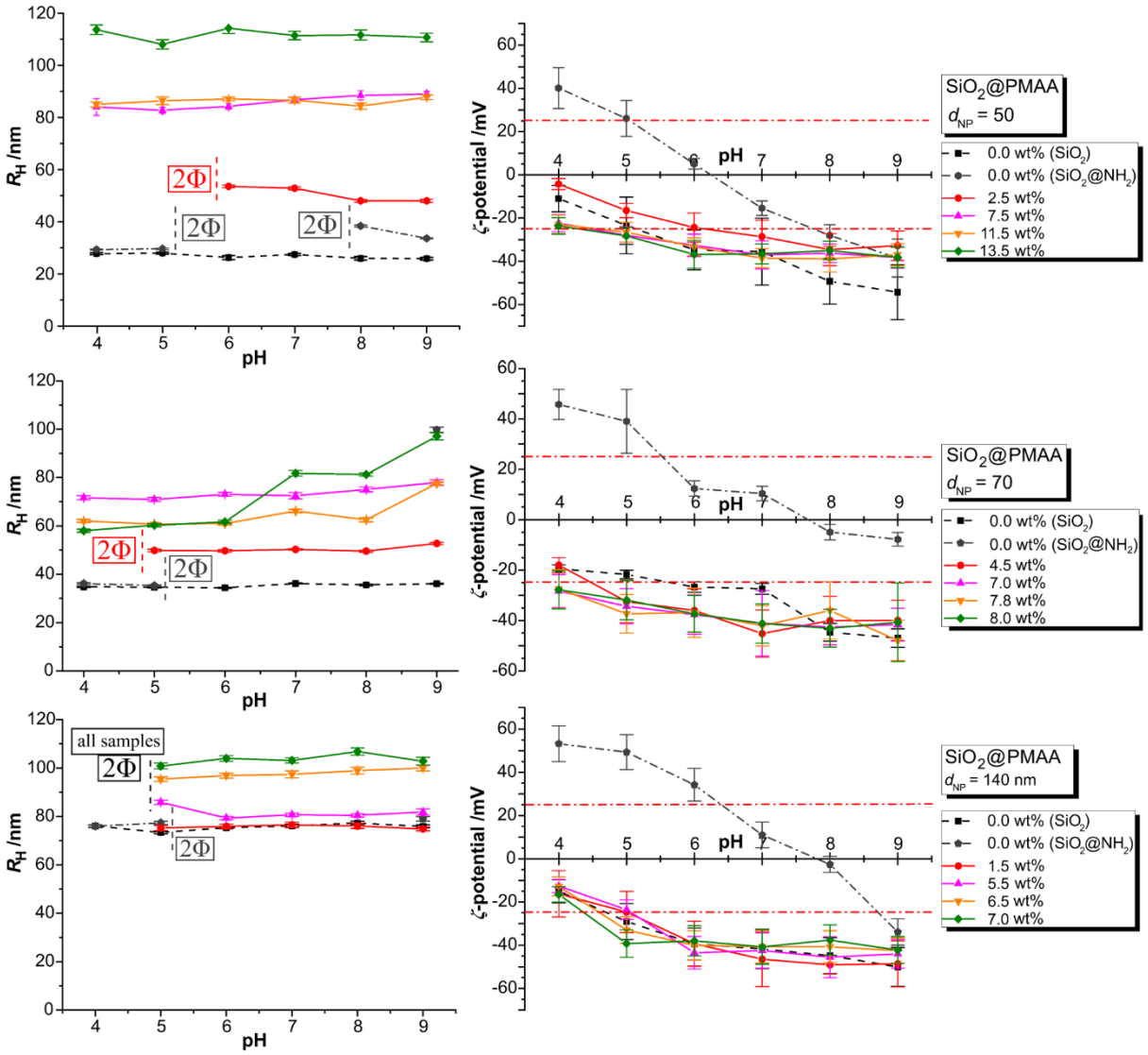

Figure S11. pH dependent values for hydrodynamic radii R_H (left) and ζ-potentials (right) for all SiO_2@PMAA-NPs (top $d = 50$ nm, middle $d = 70$ nm, bottom, $d = 140$ nm).

5 Transmission Electron Microscopy images

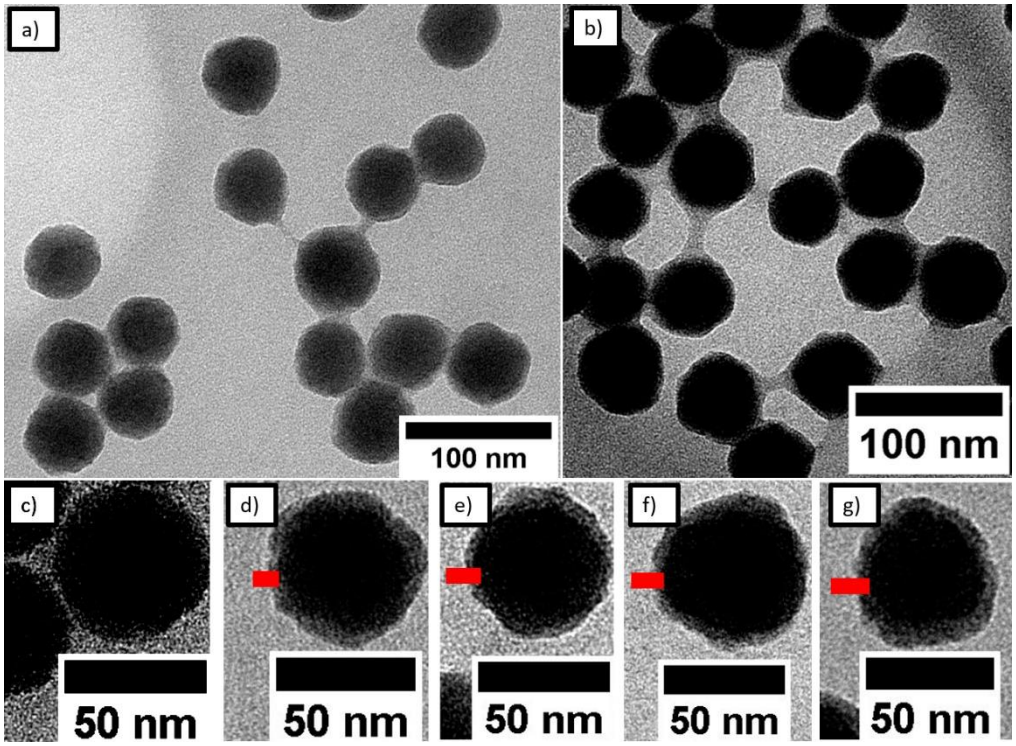

Figure S12. TEM pictures of SiO_2@PDMAEMA-NPs with core diameter d_{NP} = 50 nm: a) and b) c) As a reference SiO_2-NPs. SiO_2@PDMAEMA at different polymer grafts: d) 3.0 wt%; e) 5.5 wt%; f) 7.0 wt%; g) 11.5 wt%. For a better distinction between polymer and SiO_2 the contrast was enhanced using the software Image J. Scale bar in red demonstrate the shell thickness calculated from modeling the SANS data in full contrast conditions.

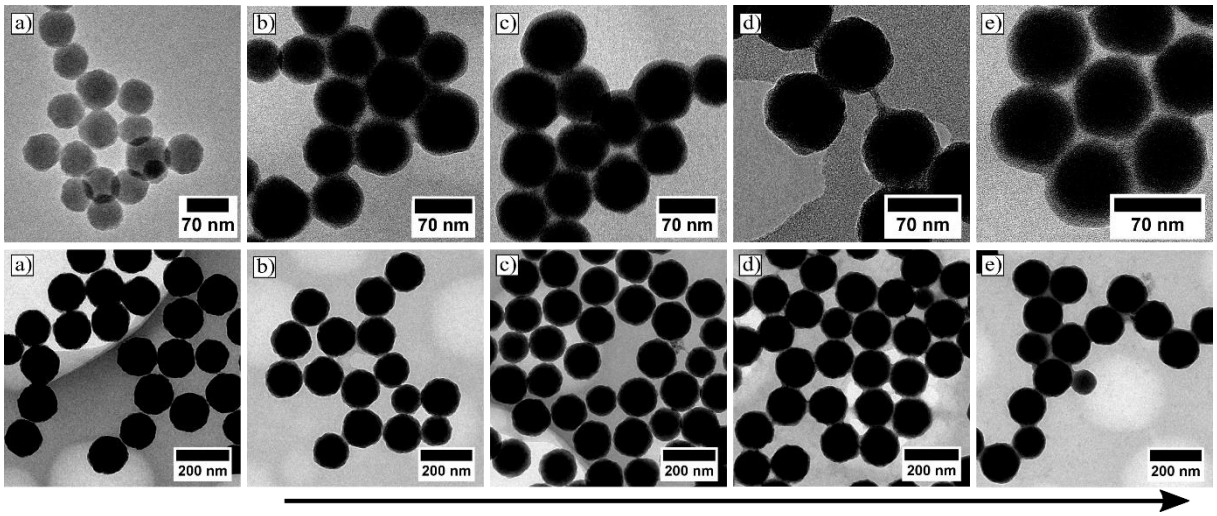

Figure S13. Larger SiO_2@PDMAEMA-NPs with different amount of grafted polymer. Top: d_{NP} = 70 nm: polymer grafting content: b) 17.5 wt%, c) 20.5 wt%, d) 23.5 wt%, e) 28.5 wt%; bottom: d_{NP} = 140 nm: polymer grafting content: b) 27.5 wt%, c) 28.0 wt%, d) 31.5 wt%, e) 33.5 wt%; a) SiO_2 as reference and from b–>e the amount of grafted polymer increases. For a better distinction between polymer and SiO_2 the contrast was enhanced using the software Image J.

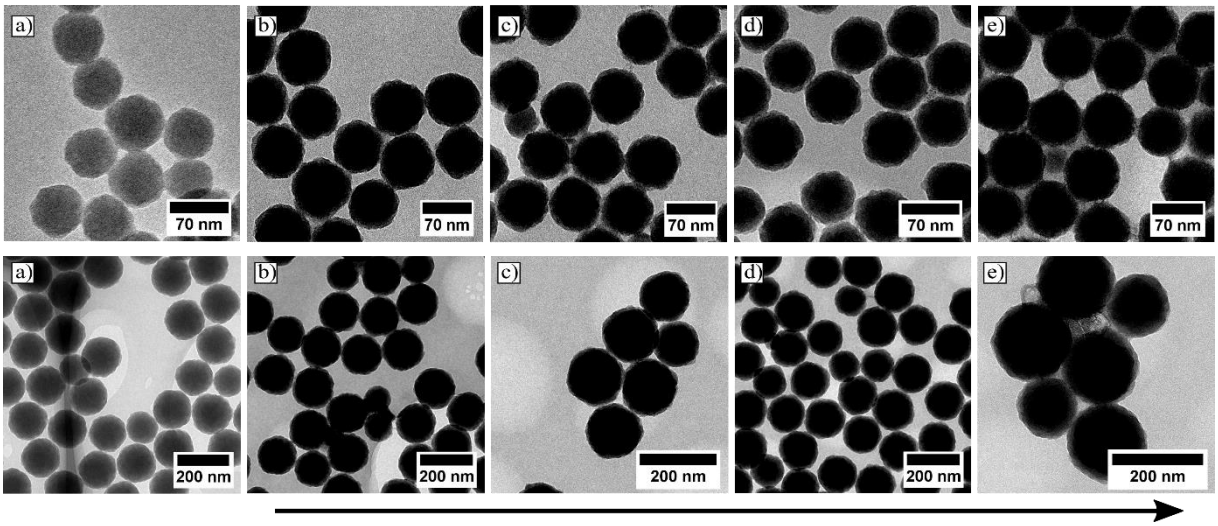

Figure S14. Larger SiO_2@PMAA-NPs with different amount of grafted polymer. Top: d_{NP} = 70 nm: polymer grafting content: b) 4.5 wt%, c) 7.0 wt%, d) 13.0 wt%, e) 13.5 wt%; bottom: d_{NP} = 140 nm: polymer grafting content: b) 1.5 wt%, c) 4.5 wt%, d) 6.5 wt%, e) 7.0 wt%; a) SiO_2 as reference and from b–>e the amount of grafted polymer increases. For a better distinction between polymer and SiO_2 the contrast was modified using the software Image J.

6 Polymerization hypothesis for PDMAEMA

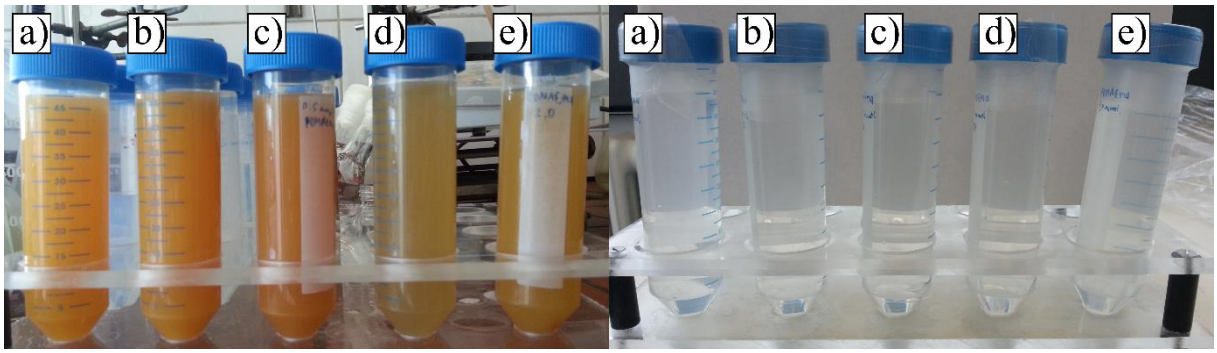

Figure S15. SiO_2@PDMAEMA-NPs with core size of d_{NP} = 50 nm. a) Left) NPs are separated from reaction mixture by centrifugation with subsequent methanol washing (2 x) and final transfer into Millipore water (neutral conditions). Right) NPs dialyzed in acetic acid-water solution (pH 4) with subsequent sonication treatment.

After the reaction SiO_2@PDMAEMA-NPs were purified by washing the remaining monomer from the NPs away with methanol and finally the NPs were transferred into Millipore water solution. Just by optical observation SiO_2@PDMAEMA-NPs have an intense orange color and with increasing amount of grafted polymer a brown tint becomes increasingly observable. The intense color disappears and a clear transparent solution is formed once the NPs were dialyzed at lower pH (~ pH 4, acetic acid) and then the NPs can easily be dispersed by sonication. We assume that the orange color has its origin in the complexation of copper(I) by the polymer. Once a certain degree of polymerization is reached the chain will start to chelate the copper by replacing the ligand PMDETA with the polymer PDAEMA. The chain thereby deactivates the initiator and therefore further monomer propagation on that chain is no longer possible. The remaining monomer is more

likely to be involved in starting a new chain on the surface of the SiO2-NP and growth of new chains on yet dormant initiator moieties takes place. As an outcome the grafting density would increase with increasing monomer concentration, thereby explaining the experimentally observed behavior.

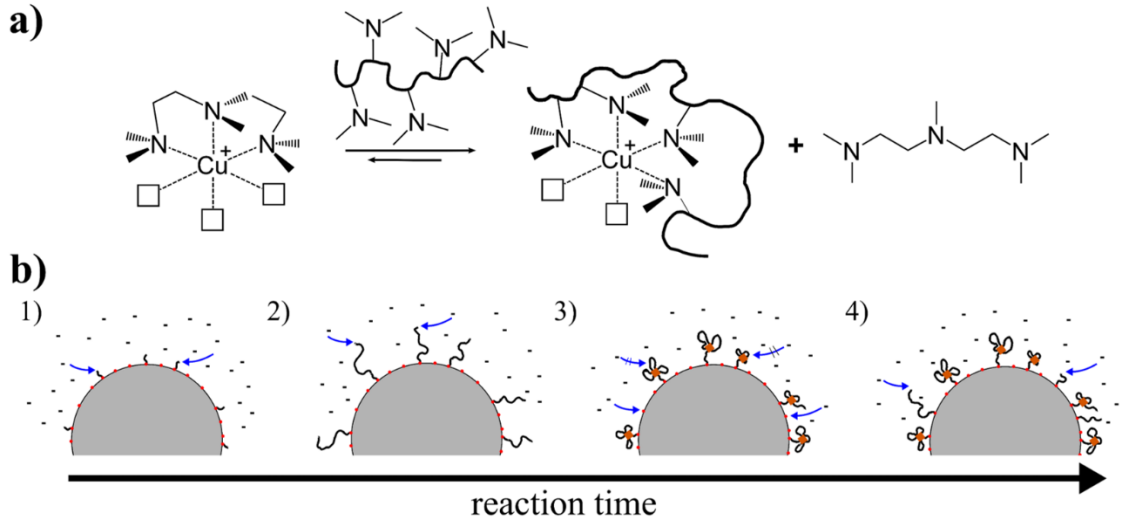

Figure S16. a) Schematic description of the chelating reaction of PDMAEMA that replaces PMDETA in the complexation of Cu^{+}. PDMAEMA can chelate up to six coordination positions of the copper complex. Presumably the chelating is not favored until 4 or more coordination positions will be occupied by the amino moiety of PDMAEMA. Once chelated the chain will contract and then further monomer propagation is impeded and no longer possible on the same chain due to steric repulsion b) 1–3) Shows sketch of the monomer propagation untill the critical degree of polymerization is reached and then 4) due to steric repulsion new chains begin to propagate.

Presumably both copper species, Cu(I) and Cu (II), will be chelated by the polymer. But just by optical inspection we think that Cu(I) is more likely complexed than Cu(II) otherwise we would see a light blue color as reported by Kavaklı et al.[41] Due to the very high copper/monomer to initiator ratio, the trapping of copper will have a weak influence on the K_{ATRP} shift from active to dormant state (note that the total dissolved copper concentration reduces constantly with increasing reaction time). In principal, up to 6 coordination sites can be occupied by the polymer. However entropically it might be favored if only four di-methyl amino moieties of one polymer chain will complex the copper. That allows for the possibility of additional complexation of two or more polymer chains at the same copper atom leading to interpolymer bridging or even interparticulate bridging. That may explain the strong turbidity of those colloidal solutions before the "orange polymer" of the NP will be charged at low pH, thereby indicating that the strong turbidity results from huge macroscopic structures.

The complex can break down by charging the di-methyl amino moiety of the polymer and the intense orange color disappears. The protonated amino groups will no longer be able to complex and instead electrostatically stabilized colloidal solutions are formed. However, the correct choice of the acid is important as the counterion has a significant influence on the brush conformation and charging. The polyelectrolyte brush charging and the copper removal by dialyzing the brush grafted NPs is much more effective with following acids from left to right: CH_3COOH > HCl > HBr. We tested all mentioned acid types, and CH_3COOH showed the fastest color transfer from orange to transparent.

To confirm our hypothesis of the grafting density increase being mediated by the copper complexation by PDMAEMA we studied the copper concentration as a function of the amount of grafted polymer. Higher

amounts of polymer correlate with more chains per particle and this is proportional to the amount of copper which can be complexed. Drying the SiO_2@PDMAEMA@Cu-agglomerates without further purification and a subsequent combined SEM-EDX analysis of those agglomerates keeping X-ray irradiation area constant confirms an increased copper amount with increasing grafted polymer (Figure D). The normalized count rate Cu K_α and K_β to Si confirms our hypothesis of the influence of copper on the grafting density.

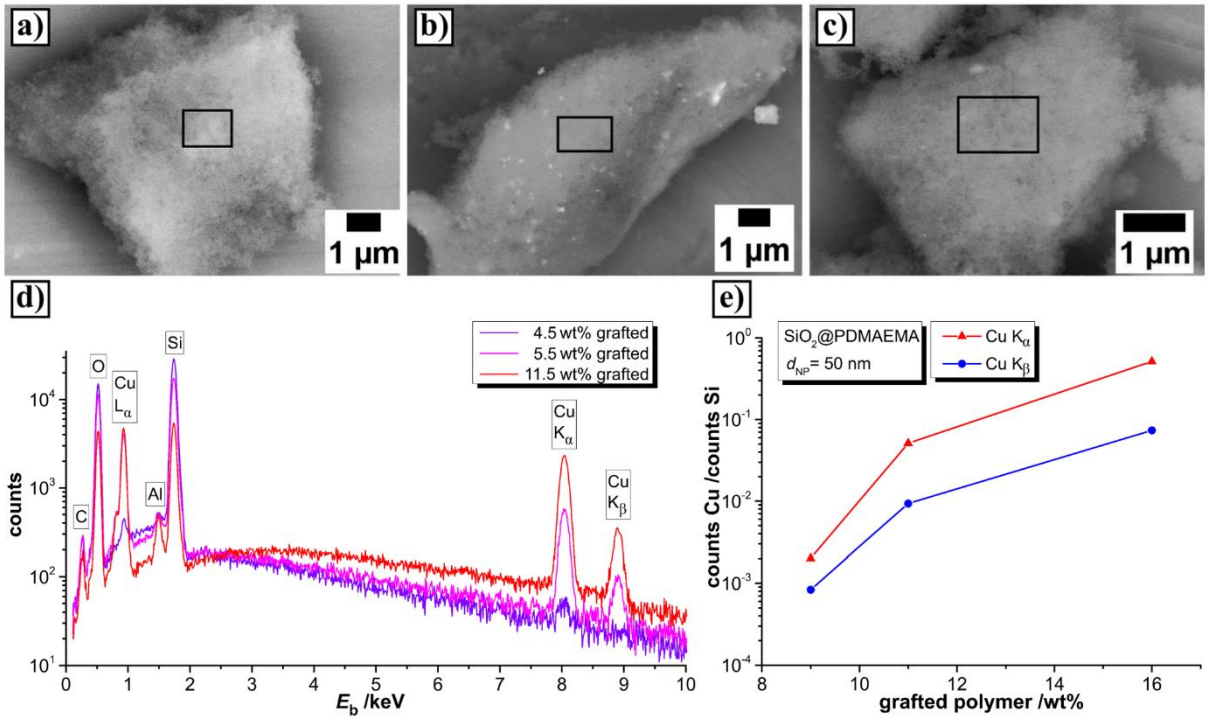

Figure S17. a–c) SEM-images of SiO_2@PDMAEMA@Cu-aggregates with the smallest core sizes d_{NP} = 50 nm for different amounts of grafted polymer: a) 4.5, b) 5.5 and c)11.5 wt%. Visualization of the excitation area for local EDX-analysis as dark rectangles. The area was tried to be kept constant as much as possible. d) Show the corresponding EDX spectra of SiO_2@PDMAEMA@Cu-aggregates for different amounts of grafted polymers and e) normalized Cu K_α and K_β versus the Si count rate as a function of grafted polymer.

In addition, in some TEM-pictures those copper complexes may be observed and interpreted as random dark dots within the polymer shell. All samples from TEM analysis were purified using dialysis but in the minority of core-shell structures the charging of the polymer may be incomplete. Nonetheless the majority of those NPs show a perfect core-shell structure without dark dots as can be seen in section 5. Those black spots result from a low transmission of heavy elements (high electron density) attributed to copper.

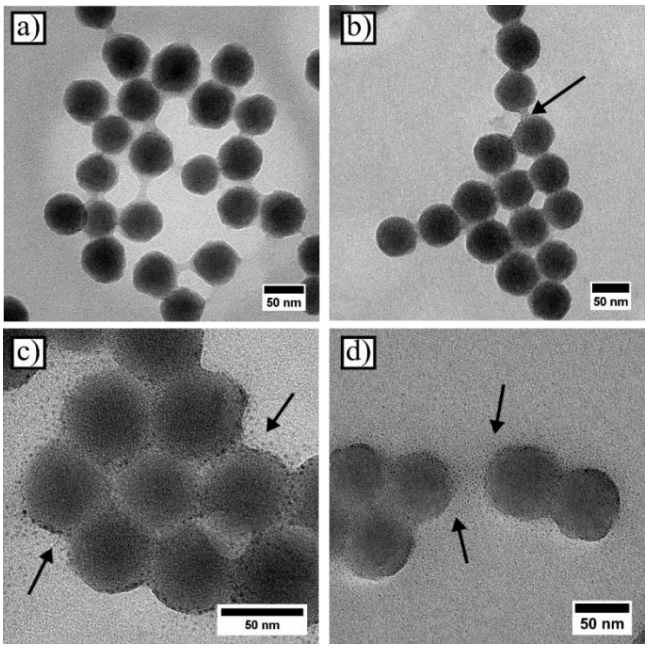

Figure S18. TEM-images of SiO_2@PDMAEMA-NPs of d = 50 nm with different amounts of grafted polymer. a) reference sample as core-shell-NPs (SiO_2@PDMAEMA with 5.5 wt% graft) without Cu-complexes where the polymer can be seen as a light grey shell surrounding the SiO_2-core., b–d) samples showing occasional dark areas within the polymer shell. For clarification the dark areas are marked with arrows.

7 SANS

7.1 Form factor model

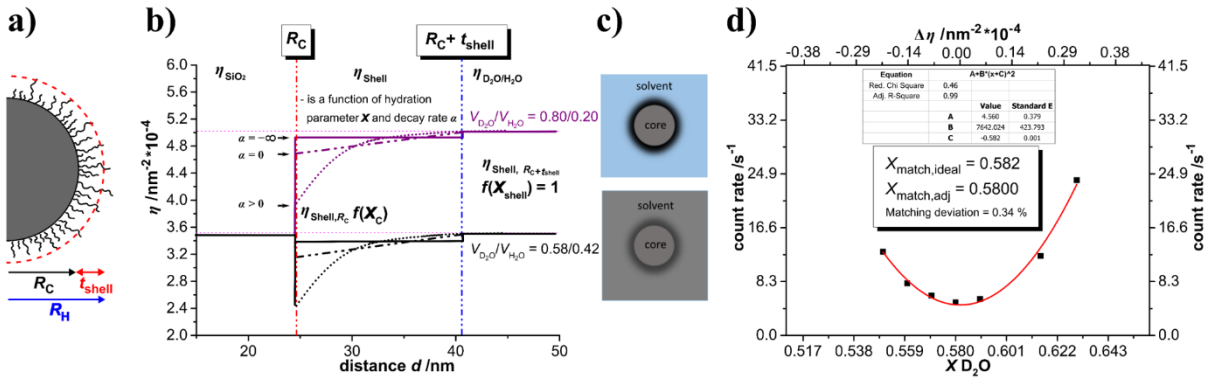

Figure S19. a) cartoon of polymer grafted NPs where unique polymer chains have different chain lengths resulting in a polymer density profile decaying exponentially. b) Scattering length density η profile for a spherical core-shell form factor model with different decaying shell profiles (purple (top): η_{shell} profile for V_{D2O}/V_{H2O} = 0.80/0.20 as an example for full contrast conditions and dark (bottom): η_{shell} profile for V_{D2O}/V_{H2O} = 0.58/0.48 as an example for CM-condition, c) schematic contrast cartoon related to the purple and dark η_{shell} profile and in d) neutron count rate (SD = 34 m) plotted as a function of the volume fraction of D_2O for bare SiO_2 NPs of radius 24.3 nm.

The SLD profile of the core-shell η_{shell} can be described as follows:

$$\eta_{\mathrm{CoreExpShell}}(t_{\mathrm{shell}}, R_C, \alpha, \eta_C, X_C, X_{\mathrm{shell}}) = \begin{cases} \eta_C & d < R_C \\ \eta_{\mathrm{Shell}} & R_C < d < R_C + t_{\mathrm{shell}} \\ \eta_{\mathrm{solv}} & d > R_C + t_{\mathrm{shell}} \end{cases} \quad \text{(S3)}$$

$$\eta_{\text{shell}}(d) = \begin{cases} \eta_{\text{shell},R_C} + \left(\eta_{\text{shell},R_C+t_{\text{shell}}} - \eta_{\text{shell},R_C}\right) d \cdot \exp(1-d)\cdot\alpha & \alpha < 0 \\ \eta_{\text{shell},R_C} - \eta_{\text{shell},R_C+t_{\text{shell}}}(1-d)\cdot\exp(-d\alpha) + \eta_{\text{shell},R_C+t_{\text{shell}}} & \alpha > 0 \end{cases} \quad \text{(S4)}$$

where d is the radial distance of the shell from the core, $\eta_{\text{shell,RC}}$ is the shell SLD at the core radius R_C, $\eta_{\text{Shell,RC+tshell}}$ is the outer shell SLD at the solvent and α describes the parameter for the exponential change of the scattering length density of the shell. The effective scattering length density of the polymer shell at the core and shell thickness $\eta_{\text{shell,RC}}$ and $\eta_{\text{shell,tshell}}$ are:

$$\eta_{\text{shell},R_C} = \left[X_C \cdot \eta_{\text{solv}} + (1 - X_C)\eta_{\text{polymer}}\right] \quad \text{(S5)}$$

$$\eta_{\text{shell},t_{\text{shell}}} = \left[x_{\text{shell}} \cdot \eta_{\text{solv}} + (1 - X_{\text{shell}})\eta_{\text{polymer}}\right] \quad \text{(S6)}$$

with X_C is volume fraction of water at the core radius and X_{shell} is volume fraction of water at the shell thickness and is set to $X_{\text{shell}} = 1$ due to smooth decay η_{shell} of the polymer shell to the solvent (Fig. 1). Then R_C+t_{shell} equation 5 simplifies in:

$$\eta_{\text{shell},t_{\text{shell}}} = [\eta_{\text{solv}}] \quad \text{(S7)}$$

Respecting the scattering length densities of solvent $\eta_{\text{D2O/H2O}}$, polymer shell η_{shell} and core η_{core} the SLD diffuse of the shell is defined:

- $\alpha > 0$ exponential decay of the SLD shell profile decay
- $\alpha = 0$ linear decay of the SLD shell profile
- $\alpha < 0$ reversed exponential decay of the SLD shell profile decay
- $\alpha \rightarrow -\infty$ constant SLD till t_{shell} then 0

The scattering intensity for radial symmetric density profile η_{Shell} can be calculated by the integral:

$$I_{\text{ExpShell}}(q) = \int_0^\infty 4\pi d^2 \frac{\sin(qd)}{qd} \eta_{Shell}(d)dd \quad \text{(S8)}$$

The scattering intensity of the core $I_{\text{sphere}}(q,R_C)$ is calculated using the spherical form factor as follows:

$$I_{\text{sphere}}(q, R_C) = K^2(q, R_C, \Delta\eta) = \left(\frac{4}{3}\pi R_C^3 \Delta\eta \cdot 3\frac{\sin(qR_C) - qR_C\cdot\cos(qR_C)}{(qR_C)^3}\right)^2 \quad \text{(S9)}$$

where q is the scattering vector, R_C the core radius of the sphere and $\Delta\eta$ the scattering length density between particle and matrix.

The particle number density is calculated via

$$^1N = \frac{c_g \cdot N_A}{M_{W,NP}} \quad \text{(S10)}$$

with c_g as weight concentration, N_A Avogadro number, $M_{W,NP}$ molecular weight of the nanoparticles. Note that ^1N have the units in $cm^{-1}\cdot nm^{-2}$.

7.2 SLD values estimation

For calculating the SLD values for the polyelectrolyte a net degree of ionization of a single polyelectrolyte chain was measured via titration $\alpha_{B,DMAEMA}$ = 0.97 for PDMAEMA at pH4 and $\alpha_{B,PMAA}$ = 0.90 for PMAA at pH 9 and assumed to be equal as in a polymer brush which in reality could be more complicated.[32] Density of PMAA was assumed as structural similar polymer PMMA, which have a measured density of ρ_{PMAA} = 1.19 g/cm^3.[33] Density of PDMAEMA was measured with a value of ρ_{DMAEMA} = 1.19 g/cm^3.

Due to the deprotonation and protonation potential of both polymers the exact $\eta_{polymer}$ is difficult to estimate precisely. For PDMAEMA and PMAA we made the following assumptions for different contrast conditions.

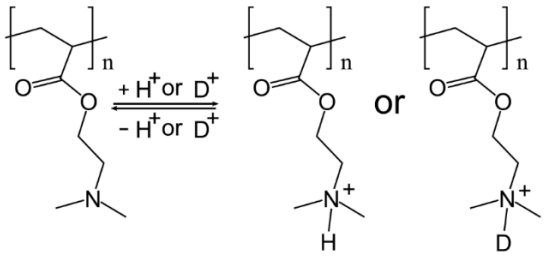

Figure S20. Shown is the protonation equilibrium for PDMAEMA in a H_2O/D_2O mixture.

From the SLD calculator provided from NIST η values are calculated:

$\eta_{PDMAEMA} = 0.945 \cdot 10^{-4}\ nm^{-2}$

$\eta_{PDMAEMA,H^+} = 0.752 \cdot 10^{-4}\ nm^{-2}$ (protonated)

$\eta_{PDMAEMA,D^+} = 1.216 \cdot 10^{-4}\ nm^{-2}$ (deuterated)

We used H_2O/D_2O mixtures, so an H to D exchange can occur. Depending on the solvent ratio, now assuming D_2O/H_2O (V/V = 0.58/0.42), the average $\eta_{PDMAEMA,H^+,D^+}$ was assumed to be given as:

$$\eta_{PDMAEMA_{H^+,D^+}} = V\%_{H^+} \cdot \eta_{PDMAEMA_{H^+}} + V\%_{D^+} \cdot \eta_{PDMAEMA_{D^+}} \quad (S11)$$

$$\eta_{PDMAEMA_{H^+,D^+}} = 0.58 \cdot 1.216 \cdot 10^{-4} nm^{-2} + 0.42 \cdot 0.752 \cdot 10^{-4} nm^{-2} = 1.0211 \cdot 10^{-4}\ nm^{-2} \quad (S12)$$

Due to very high counter ion concentration in the brush, the degree of protonation in a brush is lower than in solution. Here we assume 97% degree of ionization at pH 4 ($pKa_{PDMAEMA} \sim 7.4$) so the resulting SLD at pH 4 is:

$$\eta_{PDMAEMA_{H^+,D^+}} = 0.97 \cdot 1.0211 \cdot 10^{-4}\ nm^{-2} + 0.03 \cdot 0.945 \cdot 10^{-4}\ nm^{-2} = 1.0188 \cdot 10^{-4}\ nm^{-2} \quad (S13)$$

Same calculation were done for PMAA, assuming a degree of ionization of 0.9 for PMAA brushes. The scattering densities are summarized for different solvent conditions in Table S6.

Table S6. Scattering length densities of used polymers in different solvent conditions with high or low degree of ionization.

material	Sum formula added in NIST	ρ [g/cm^{-3}]	D_2O/H_2O (V/V)	SLD [nm^{-2}] ·10^{-4}
SiO_2	SiO_2	2.2	–	3.4750
PDMAEMA (protonated, D_2O)	$C_7H_{13}NO_2D$	1.19	0.80/0.20	1.1178
PDMAEMA (protonated, CM)	$C_7H_{14}NO_2$	1.19	0.58/0.42	1.0188
PDMAEMA (deprotonated, dry)	$C_7H_{13}NO_2$	1.19	–	0.9450
PMAA (protonated, D_2O)	$C_4H_5O_2D$	1.19	0.80/0.20	1.9856
PMAA (protonated, CM)	$C_4H_6O_2$	1.19	0.58/0.42	1.8003
PMAA (deprotonated, D_2O)	$C_4H_5O_2$	1.19	–	1.6736
PMAA (deprotonated, CM)	$C_4H_5O_2$	1.19	–	1.6578
D_2O/H_2O (V/V = 0.8/0.2)	–	1.08	–	5.0034
D_2O/H_2O (V/V = 0.58/0.42)	–	1.05	–	3.4748

Full contrast condition = (V_{D2O}/V_{H2O} = 0.8/0.2); contrast match conditions (CM) (V_{D2O}/V_{H2O} = 0.58/0.42)

The density of the polymer was estimated by measuring the density of identically synthesized PDMAEMA solution (same reaction conditions except they were not surface initiated, but the polymerization took place in solution) at several concentrations and approximated to pure polymer from the linear extrapolation with the density for PDMAEMA $\rho_{PDMAEMA}$ = 1.19 g/cm^3.

The values for η were used to calculate the scattering intensities.

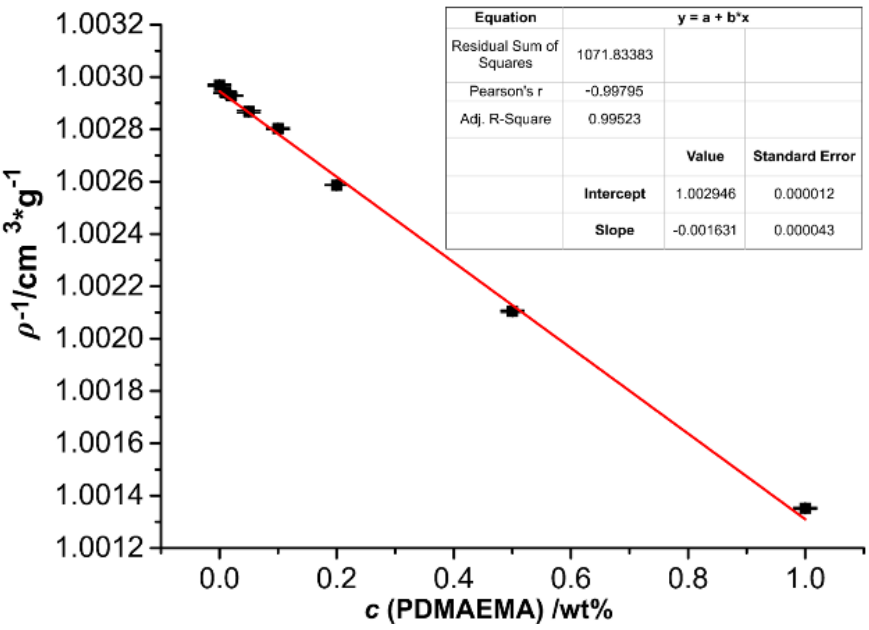

Figure S21. reciprocal densities plotted as a function of the PDMAEMA concentration in wt%.

With:

$$\rho = \frac{1}{y} = \frac{1}{(a+b\cdot x)} = \frac{1}{1.002946\frac{\mathrm{cm}^3}{\mathrm{g}} - 0.001631\frac{\mathrm{cm}^3}{\mathrm{g}}\cdot 100\,\%} = 1.19\,\frac{\mathrm{g}}{\mathrm{cm}^3}$$

The degree of ionization was obtained via titration of both polymers. PMAA sodium salt is a commercial polymer (Sigma Aldrich) with a molecular weight of 5100 g/moL (degree of polymerization = 51). The self synthesized PDMAEMA was taken, where molecular weight and degree of polymerization are unknown.

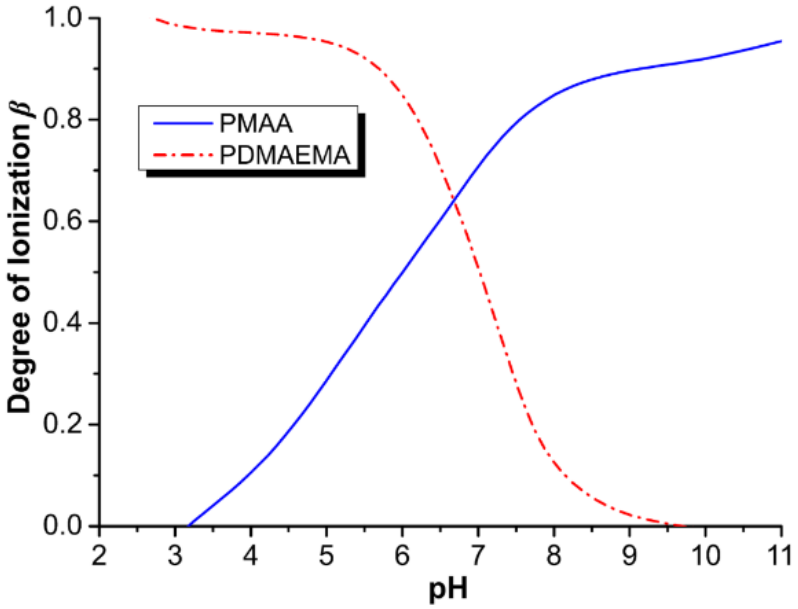

Figure S22. Measured degree of ionization β of PDMAEMA and PMAA at different pH values.

7.3 SANS-data of SiO_2-NPs at full contrast conditions

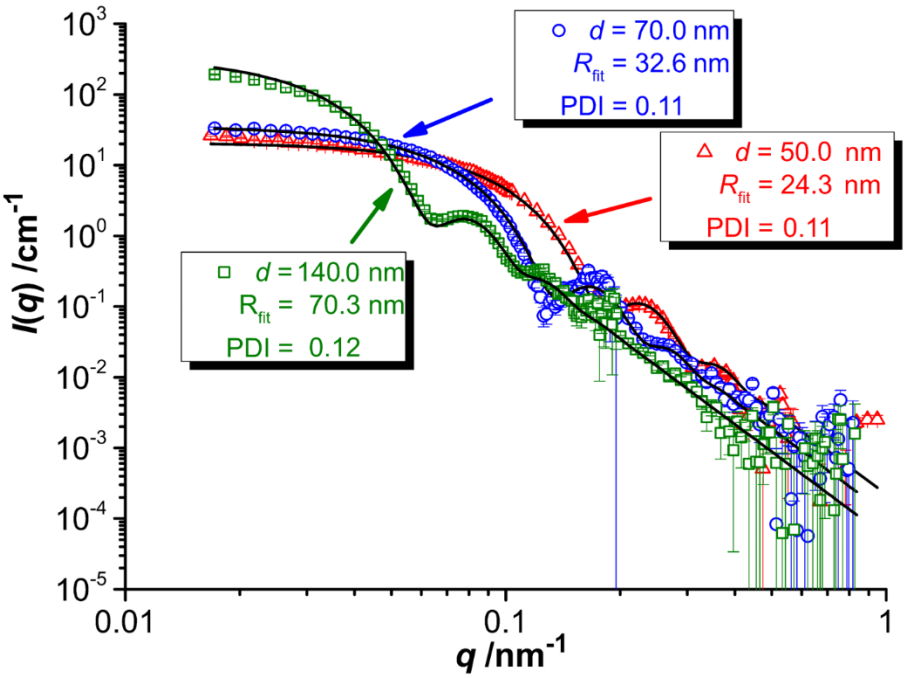

Figure S23. SANS data (dots) of pure silica nanoparticles with corresponding sphere form factor fit (dark line). Data for the smallest particles is measured at KWS-1 and for the bigger particles at D11.

7.4 SANS-data of SiO_2@PDMAEMA d = 50

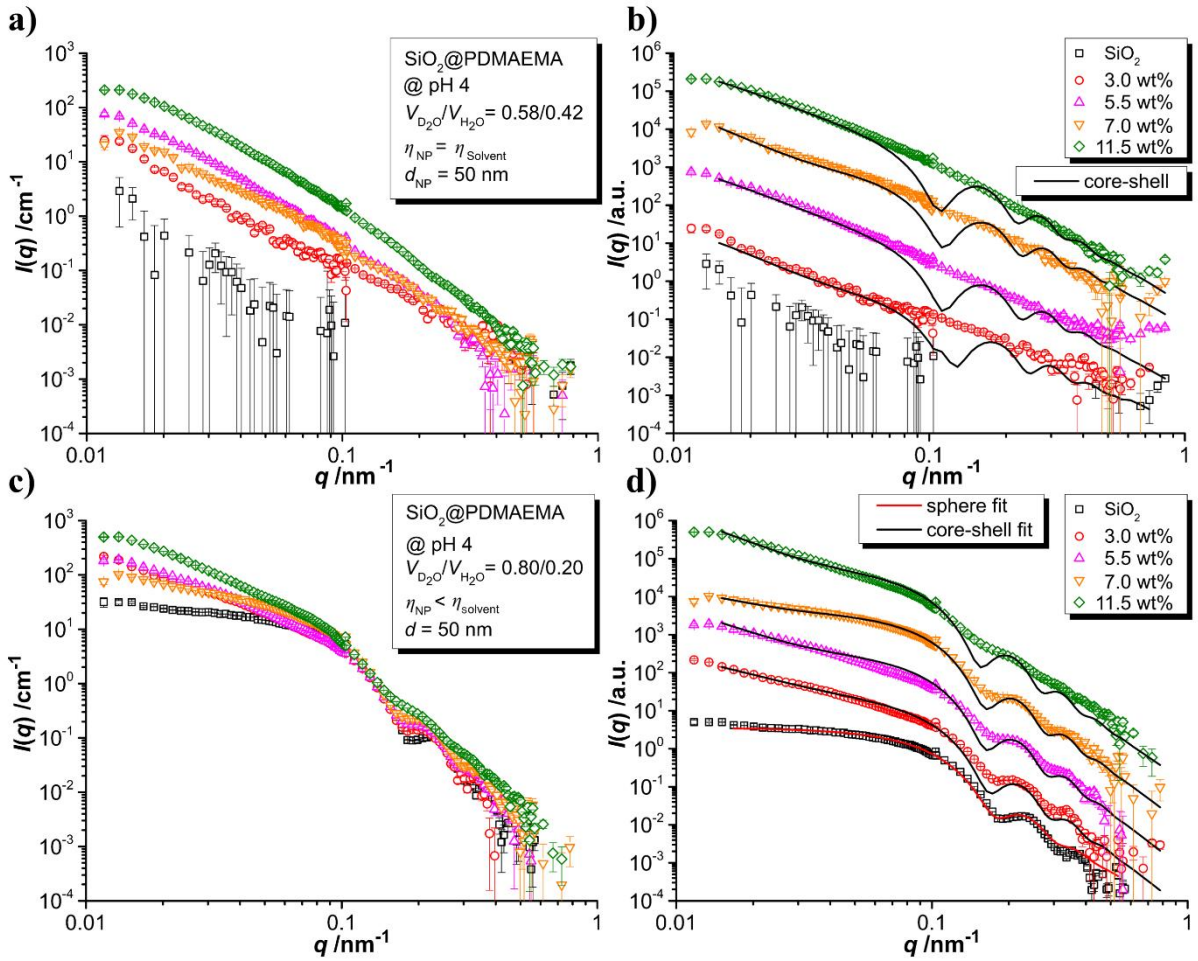

Figure S24. SiO_2@PDMAEMA for d = 50 nm at a,b) $\eta_{core} = \eta_{solvent}$ and c,d) $\eta_{core} < \eta_{solvent}$ conditions at pH 4. The data is shown in absolute scale (left) and for better legibility shifted with a cumulative factor of 10 for each scattering curve (right). Modeled scattering intensities are shown as dark lines for polymer grafted nanoparticles and as a red line for silica nanoparticles. Data measured at KWS-1.

7.5 SANS-data of SiO_2@PMAA-NPs d = 50 nm

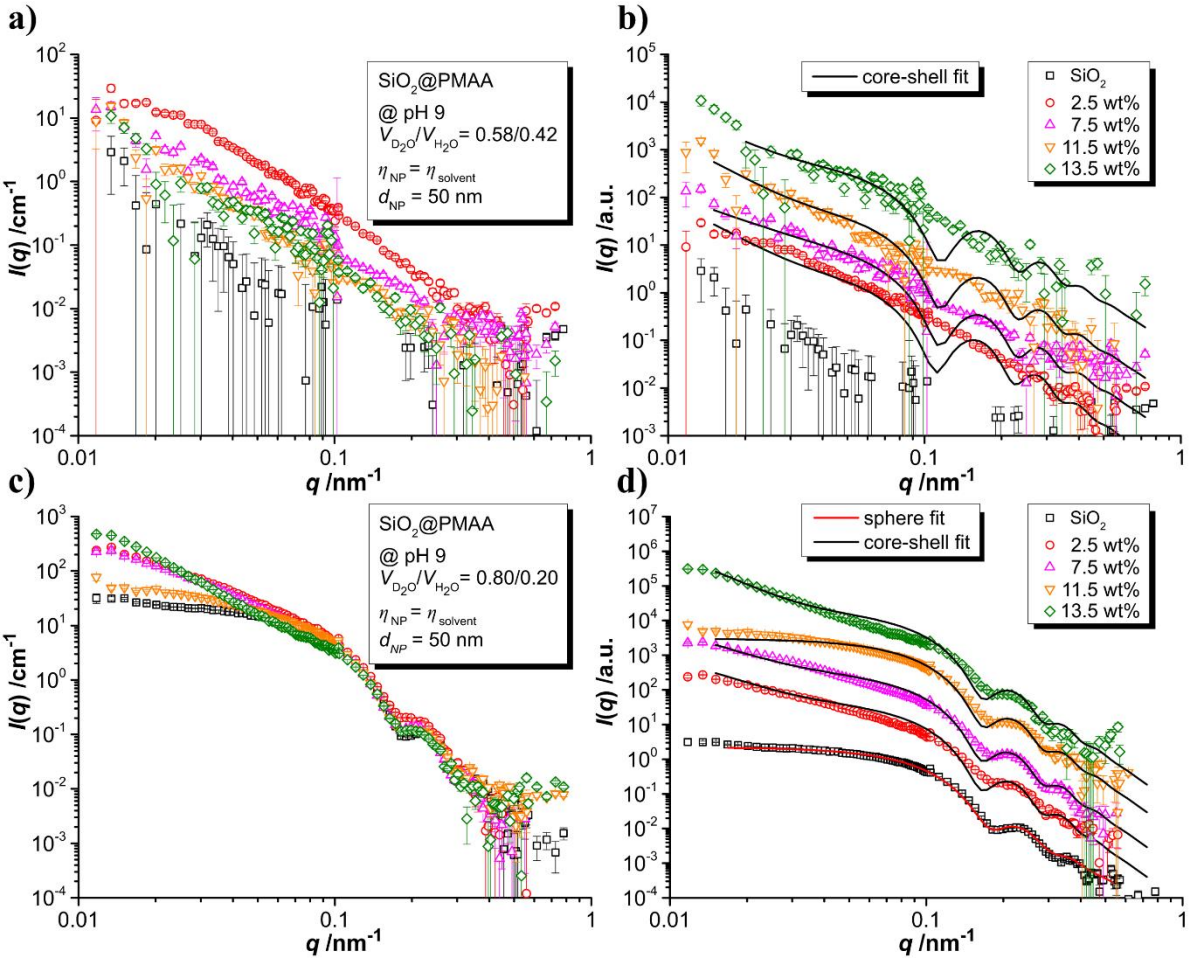

Figure S25. SiO_2@PMAA for d = 50 nm at a,b) $\eta_{core} = \eta_{solvent}$ and c,d) $\eta_{core} < \eta_{solvent}$ conditions at pH 4. The data is shown in absolute scale (left) and for better legibility shifted with a cumulative factor of 10 for each scattering curve (right). Modeled scattering intensities are shown as dark lines for polymer grafted nanoparticles and as a red line for silica nanoparticles. Data measured at KWS-1.

7.6 SANS-data of SiO_2@PDMAEMA-NPs d = 70 nm

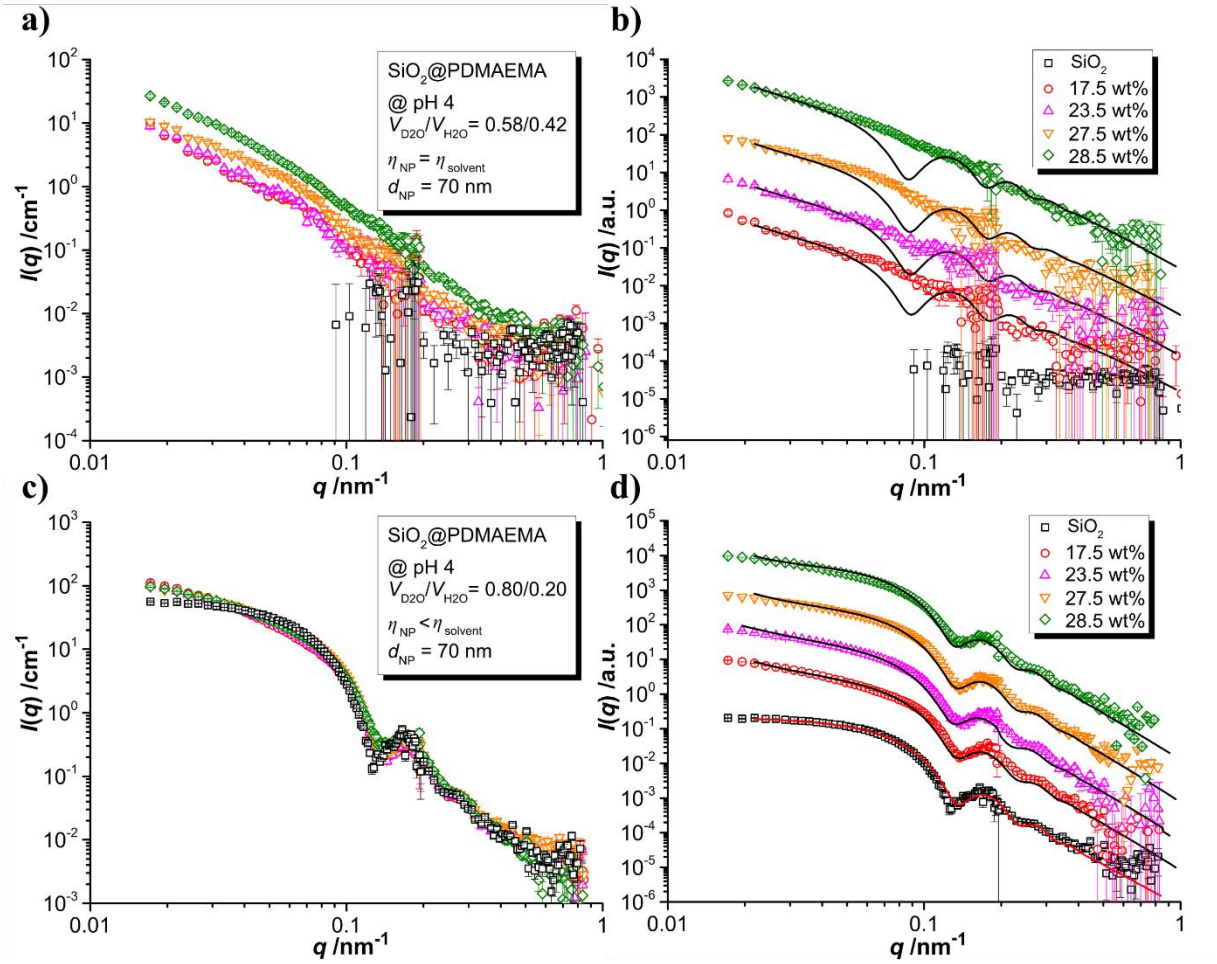

Figure S26. SiO_2@PDMAEMA for d = 70 nm at a,b) $\eta_{core} = \eta_{solvent}$ and c,d) $\eta_{core} < \eta_{solvent}$ conditions at pH 4. The data is shown in absolute scale (left) and for better legibility shifted with a cumulative factor of 10 for each scattering curve (right). Modeled scattering intensities are shown as dark lines for polymer grafted nanoparticles and as a red line for silica nanoparticles. Data measured at D11.

7.7 SANS-data of SiO_2@PDMAEMA-NPs d = 140 nm

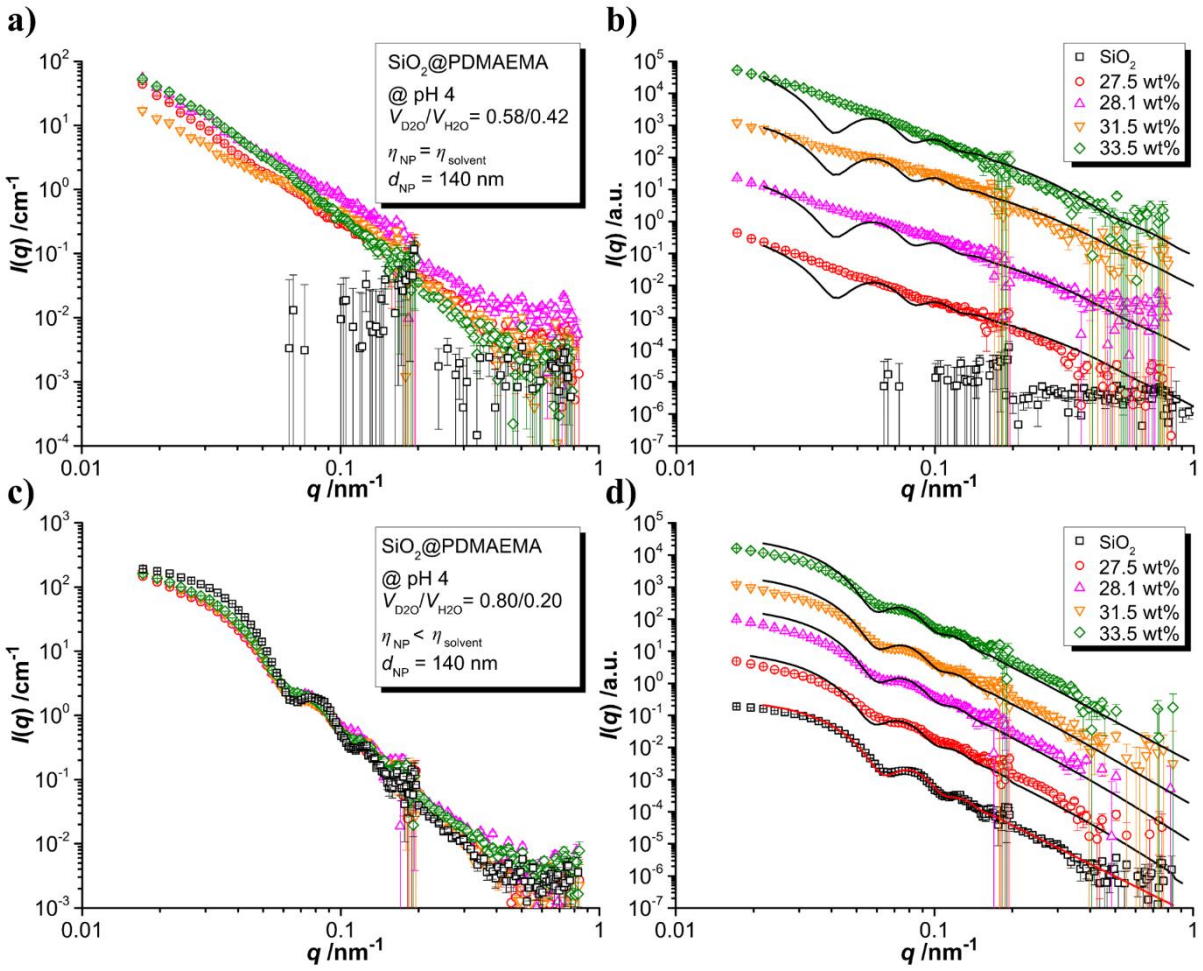

Figure S27. SiO_2@PDMAEMA for d = 140 nm at a,b) $\eta_{core} = \eta_{solvent}$ and c,d) $\eta_{core} < \eta_{solvent}$ conditions at pH 4. The data is shown in absolute scale (left) and for better legibility shifted with a cumulative factor of 10 for each scattering curve (right). Modeled scattering intensities are shown as dark lines for polymer grafted nanoparticles and as a red line for silica nanoparticles. Data measured at D11.

7.8 SANS-data of SiO_2@PMAA-NPs d = 140 nm

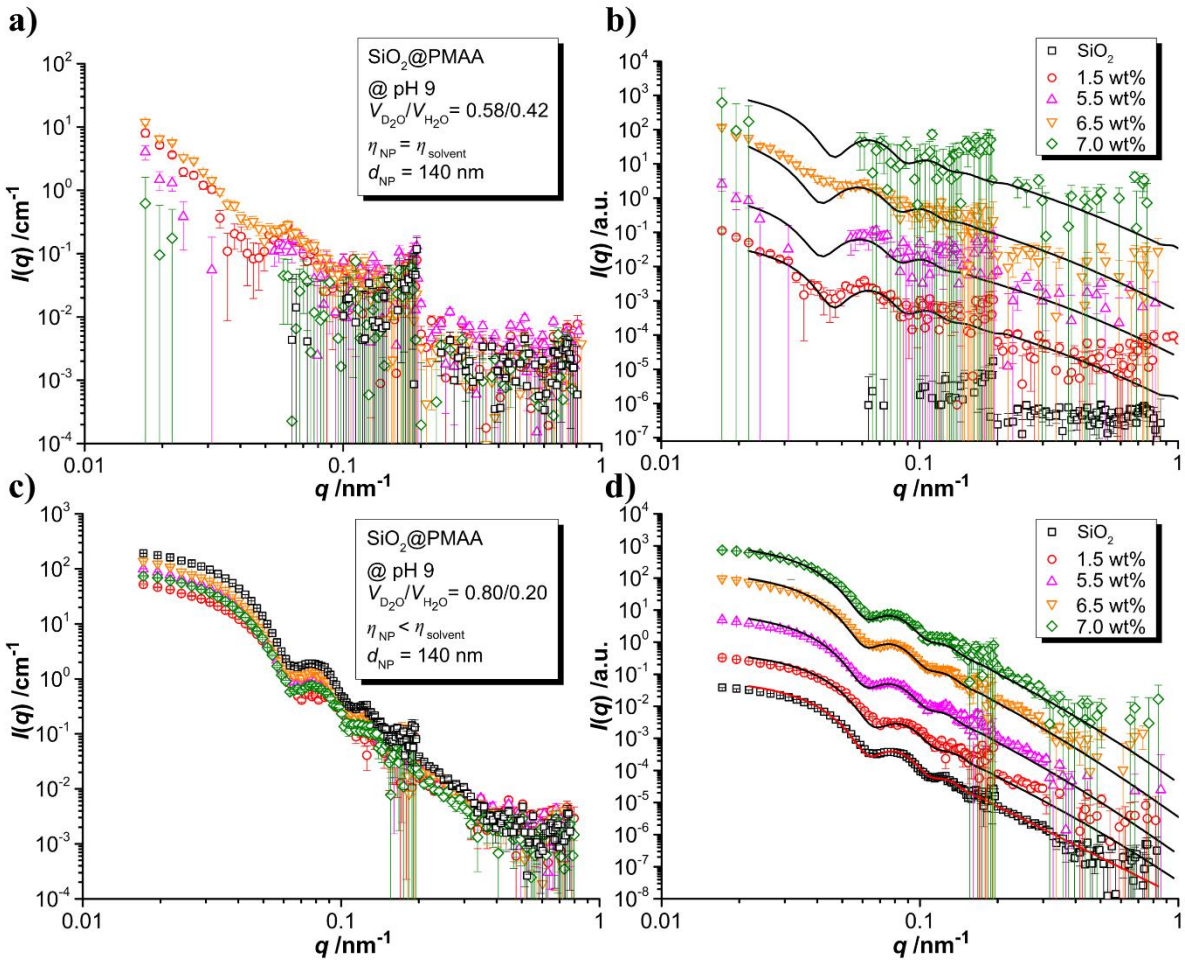

Figure S28. SiO_2@PMAA for d = 140 nm at a,b) $\eta_{core} = \eta_{solvent}$ and c,d) $\eta_{core} < \eta_{solvent}$ conditions at pH 4. The data is shown in absolute scale (left) and for better legibility shifted with a cumulative factor of 10 for each scattering curve (right). Modeled scattering intensities are shown as a dark lines for polymer grafted nanoparticles and as a red line for silica nanoparticles. Data measured at D11.

Table S7. summarized values from SANS data modeling for SiO_2@PDMAEMA and SiO_2@PMAA-NPs at both contrast conditions for $d = 70$ and 140 nm. For the form factor: polymer graft content $X_{polymer}$, weight concentration c_g, particle number density ^1N, shell thickness t_{shell}, polymer volume fraction at the core radius X_C, exponential decay rate a, for the structure factor: radius of individual scatterer R_{ind}, cut off size R_f and fractal dimension coefficient D_f

	$X_{polymer}$	c_g	^1N	t_{shell}	x_C	a	R_{ind}	R_f	D_f
	wt%	g/L	$cm^{-1} \cdot nm^{-2}$	nm			nm	nm	
					$\eta_{core} = \eta_{solvent}$				
SiO_2@PDMAEMA @ pH 4 $d = 70$ nm	17.5	5.8	0.139	10.6	0.55	4.43	46	171	2.63
	23.5	4.8	0.109	13.1	0.50	4.87	49	165	2.78
	27.5	5.2	0.115	14.9	0.45	5.32	50	143	2.73
	28.5	6.4	0.140	16.1	0.34	4.60	50	143	2.50
					$\eta_{core} < \eta_{solvent}$				
	17.5	2.8	0.067	10.7	0.55	13.00	48	177	2.72
	23.5	2.5	0.057	13.0	0.50	13.00	48	128	2.64
	27.5	2.4	0.053	14.1	0.46	13.00	51	155	2.90
	28.5	3.3	0.072	16.1	0.38	13.00	52	194	3.12
					$\eta_{core} = \eta_{solvent}$				
SiO_2@PDMAEMA @ pH 4 $d = 140$ nm	27.5	1.4	0.0024	12.5	0.50	1.65	–	–	–
	28.1	1.8	0.0031	14.2	0.48	1.75	–	–	–
	31.5	1.4	0.0023	15.4	0.43	2.03	–	–	–
	33.5	2.6	0.0043	15.6	0.30	1.07	–	–	–
					$\eta_{core} < \eta_{solvent}$				
	27.5	0.7	0.0012	12.1	0.54	6.00	–	–	–
	28.1	0.6	0.0010	14.1	0.48	6.60	–	–	–
	31.5	0.7	0.0011	14.5	0.42	6.00	–	–	–
	33.5	1.1	0.0018	15.1	0.30	5.00	–	–	–
					$\eta_{core} = \eta_{solvent}$				
SiO_2@PMAA@ pH 9 $d = 140$ nm	1.5	3.9	0.0083	12.3	0.51	2.43	–	–	–
	5.5	4.8	0.0099	18.4	0.52	6.95	–	–	–
	6.5	5.2	0.0106	25.2	0.48	8.35	–	–	–
	6.5	5.4	0.0109	29.0	0.52	13.63	–	–	–
					$\eta_{core} < \eta_{solvent}$				
	1.5	2.1	0.0045	11.2	0.51	6.78	–	–	–
	5.5	2.8	0.0058	18.9	0.52	7.64	–	–	–
	6.5	2.7	0.0055	26.0	0.50	9.65	–	–	–
	7.0	2.6	0.0053	29.3	0.51	14.50	–	–	–

7.9 Model fitting according to a more accurate model from Pedersen and Gerstenberg

In addition to fitting SANS data with spheres having a homogeneous core with the radius R_C and a shell with various scattering length density profiles, a model for homogeneous spherical core decorated by polymer chains with Gaussian statistics attached to its surface, as proposed by Pedersen and Gerstenberg[48] in the case of diblock copolymer micelles.

$$P_{mic}(q) = N_{agg}^2 \beta_{core}^2 F_{sphere}(qR_C)^2 + N_{agg}\beta_{brush}^2 P_{brush}(qR_G) + 2\,N_{agg}^2 \beta_{brush}\beta_{core} S_{brush|core}(q, R_C, R_G, d) + N_{agg}(N_{agg}-1)\beta_{brush}^2 S_{brush|brush}(q, R_C, R_G, d), \quad (S14)$$

where N_{agg} is the number of polymer chains attached, F_{sphere} is the form factor amplitude for spheres:

$$F_{sphere}(qR_C) = 3\frac{\sin(qR_C) - qR_C \cdot \cos(qR_C)}{(qR_C)^3}, \quad (S15)$$

P_{brush} is the form factor for Gaussian chains (Debye function):

$$P_{brush}(qR_G) = 2\frac{\exp(-(qR_G)^2) - 1 + (qR_G)^2}{(qR_G)^4}, \quad (S16)$$

and $S_{brush|core}$ and $S_{brush|brush}$ are the cross-terms:

$$S_{brush|core}(q, R_C, R_G, d) = F_{sphere}(qR_C)\frac{1-\exp(-(qR_G)^2)}{(qR_G)^2}\frac{\sin(q(R_C+dR_G))}{q(R_C+dR_G)} \text{ and} \quad (S17)$$

$$S_{brush|brush}(q, R_C, R_G, d) = \left[\frac{1-\exp(-(qR_G)^2)}{(qR_G)^2}\right]^2 \left[\frac{\sin(q(R_C+dR_G))}{q(R_C+dR_G)}\right]^2, \quad (S18)$$

where d is an adjustment parameter indicating where the Gaussian chains are starting (to avoid penetration of the core by the chains). In line with the original article of Pedersen and Gerstenberg, we kept $d = 1$. Note that for Gaussian chains $R_G = (Lb/6)^{1/2}$ where L is the contour length and b is the Kuhn length.

The contrasts and volumes are included in the β terms:

$$\beta_{brush} = SL_{brush} - SLD_{solvent}V_{brush} \quad (S19)$$

$$\beta_{core} = SL_{core} - SLD_{solvent}V_{core} \quad (S20)$$

The core radius R_C is assumed to be log-normally distributed, with the mean at R_C and a relative standard-deviation p:

$$pdf(x, R_C, p) = \frac{1}{xs\sqrt{2\pi}}\exp\left[-\frac{\ln x - \ln m}{2s^2}\right], \quad (S21)$$

with $m = \frac{R_C}{\sqrt{\ln p^2 + 1}}$ and $s = \sqrt{\ln(p^2+1)}$. The mean core radius and polydispersity are fixed from the parameters obtained from SAXS data. We assume a constant surface grafting density of polymer chains, i.e. N_{agg} scales with R_C^2.

The low q behavior of most data indicate the presence of some aggregates. This is taken into account by a fractal structure factor (see main article Eq. 6), while in addition the short range excluded volume effect from cores

sticking together in the aggregates is modelled via a polydisperse hard sphere implemented via the decoupling approximation.[49] For both structure factors, we take as a characteristic size the SiO_2 core.

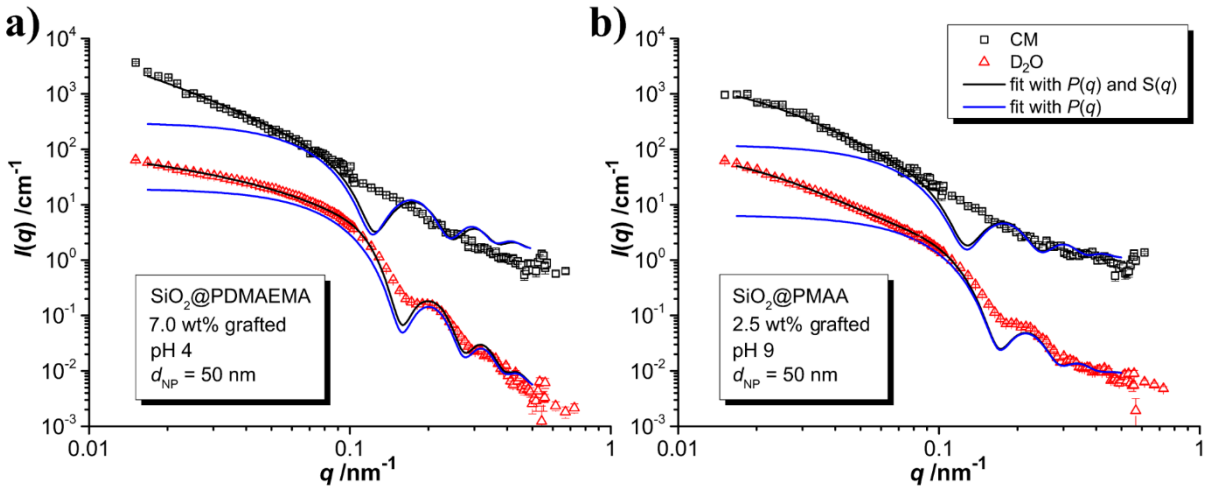

Figure S29. SANS data and corresponding modeled data according to Pedersen and Gerstenberg[48] of a) SiO_2@PDMAEMA and b) SiO_2@PMAA. The abbreviation (D_2O → $\eta_{core} < \eta_{solvent}$; CM → $\eta_{core} = \eta_{solvent}$). The data is shown in absolute scale but for a better legibility the data for CM conditions is multiplied with a factor 100. Data measured at KWS-1.

Table S8. summarized values from SANS data modeling for SiO_2@PDMAEMA and SiO_2@PMAA-NPs at both contrast conditions for d = 50 nm. Whenever possible, the same parameters are used to fit both contrast conditions, however the volume fraction of particles is different, and for PMAA the fractal dimension of aggregates is also found to be different.

Parameter explanation		unit		PDMAEMA		PMAA	
				CM	D_2O	CM	D_2O
grafting density per surface	σ	nm^{-2}	fit	0.23		0.12	
Monomer units per particle*	n		fix	72500		76700	
Volume of monomer brush	$V_{m,brush}$	nm^3	fix	0.221		0.099	
Scattering length brush	SL_{brush}	nm	fix	$3.63 \cdot 10^{-5}$		$2.41 \cdot 10^{-5}$	
gyration radius	R_G	nm	fit	1.12		0.73	
volume fraction of silica core	ϕ		fit	0.0021	0.00054	0.0065	0.0029
fractal dimension	D_f		fit	1.0	1.0	1.19	2.38
cut-off length fractal aggregate	R_f	nm	fit	123		50	
effective excluded volume fraction (short range repulsion)	fhs		fit	0.20		0.09	
deducted parameters							
average number of chains per particle	N_{agg}			2004		1048	
average number of monomer units per chain	N			36		73	

* value deducted from the TGA measurements

$\eta_C = 3.475 \cdot 10^{-4}\ nm^{-2}$, $\eta_{CM} = 3.5 \cdot 10^{-4}\ nm^{-2}$, $\eta_{D2O} = 5.0 \cdot 10^{-4}\ nm^{-2}$

R_C = 25.04 nm, PDI_C = 0.0877

In the Pedersen model aimed at modelling core-shell micelles from block copolymers, the amount of solvent in the core is considered as the core can be solvated; here we fixed this value to 0; SiO_2 NPs are known to have porosity, but changing this value did not improve the fits.